University of Sistan and Baluchestan

Challenges in Nano and Micro Scale Science and Technology

Online ISSN: 2821 - 000X

Coumarin-Conjugated Silver Nanoparticles; Potent Antibacterial and Antibiofilm Agents Against Multidrug-Resistant Pseudomonas Aeruginosa

Ensiyeh Abbaspour Naderi[1] | Seyedeh Tooba Shafighi[1]✉ | Amir Mirzaie[2] | Ali Salehzadeh[1]

1. Department of Biology, Ra.C., Islamic Azad University, Rasht, Iran.
2. Department of Biology, Pa.C., Islamic Azad University, Parand, Iran

Corresponding Author's Email: tshafighi@iau.ac.ir

Article Info

Article type:
Research Article

Article history:
Received: 2026-06-15
Received in revised form: 2026-06-21
Accepted: 2026-06-28
Published online:

Keywords:
Biofilm,
Coumarin,
Pseudomonas aeruginosa,
Silver nanoparticles,

ABSTRACT

Multidrug-resistant (MDR) Pseudomonas aeruginosa is a major health threat in the community and hospital setting. This work investigates the antibacterial and antibiofilm effects of coumarin-conjugated silver nanoparticles (Ag@Glu-Coumarin nanoparticles) on MDR P. aeruginosa. Silver nanoparticles (NPs) were initially functionalized with glucose, conjugated with coumarin and characterized by Fourier Transform Infrared Spectroscopy (FT-IR), X-ray diffraction (XRD), Field Emission Scanning Electron Microscope (FE-SEM), Energy-dispersive X-ray spectroscopy (EDS)-mapping, Dynamic Light Scattering (DLS), zeta potential and Thermogravimetric Assay (TGA) analyses. Antibacterial potential of the NPs was studied by disk diffusion and broth microdilution assays. Biofilm formation ability of P. aeruginosa strains and antibiofilm effects of Ag, coumarin and Ag@Glu-Coumarin NPs were analysed using the crystal violet staining method. The relative expression of the algD, pelA, and pslA genes was investigated by real-time PCR. The Ag@Glu-Coumarin NPs were correctly synthesized with a spherical shape and average size of 80 nanometer(nm). The surface charge and hydrodynamic size of the particles were -80.4 milliVolt (mV) and 271.2 nm, respectively and exhibited sufficient thermal stability at temperatures up to 100 °C. The average diameter of growth inhibition zones caused by Ag@Glu-Coumarin NPs was 30mm, and the minimum growth inhibitory concentration ranged 256-512µg/mL. The strains 1, 6, 7, 8 and 10 displayed the highest biofilm formation potential, which was reduced by 77.3, 75.9, 90.3, 89.2 and 89.4%, respectively, in treated bacteria. Moreover, treatment of P. aeruginosa strains with Ag@Glu-Coumarin NPs significantly reduced expression of the algD, pelA and pslA genes to 0.68, 0.46 and 0.37 folds, respectively. This study demonstrated antibacterial activity and antibiofilm effects of Ag@Glu-Coumarin NPs, suggesting their therapeutic potential against MDR P. aeruginosa strain.

1. INTRODUCTION

Pseudomonas aeruginosa is a rod-shaped, aerobic and gram-negative bacterium that is frequently found in water, soil, plants and animals. It is considered an opportunistic human pathogen causing various infections in humans such as otitis, septicemia, urinary tract infection and respiratory diseases. *P. aeruginosa* is a main cause of mortality in immunocompromised patients, burns and cystic fibrosis. This bacterium has a high ability to adapt to different environmental conditions and is highly resistant to antimicrobial compounds [1]. Development of drug resistance by *P. aeruginosa* is a main therapeutic challenge that reduces the effectiveness of antibiotic treatment interventions. Multidrug Resistant (MDR) *P. aeruginosa* is a major health threat to the human population, particularly in hospital settings. Broad spectrum of antibiotic resistance in MDR *P. aeruginosa* limits effective therapeutic options; therefore finding effective drugs against these strains is of significant priority [2].

Antibiotic resistance in *P. aeruginosa* arises from several inherent and acquired resistance determinants. In addition to low permeability of the bacterial outer membrane and multidrug efflux systems, which account for bacterial intrinsic drug resistance mechanisms, biofilm formation is regarded as a main determinant factor in the antibiotic resistance of *P. aeruginosa*. Biofilm consists of a bacterial population embedded in a self-produced extracellular polymeric matrix established on living and non-living surfaces. In biofilm growth, bacteria typically show significantly higher resistance to antimicrobials, as

How to Cite this paper: Abbaspour Naderi E. Shafighi S.T. Mirzaie A. Salehzadeh A. Coumarin-conjugated silver nanoparticles; potent antibacterial and antibiofilm agents against Multidrug-resistant Pseudomonas aeruginosa. *Challenges in Nano and Micro Scale Science and Technology*. 2026; 14(2): 57-67. DOI: 10.22111/cnmst.2026.55806.1310

 Publisher: University of Sistan and Baluchestan.
DOI: 10.22111/cnmst.2026.55806.1310

the biofilm matrix acts as a barrier that reduces bacterial exposure to the drugs. Furthermore, bacteria that grow in biofilm exhibit different phenotypic characteristics compared with planktonic growth, noticeably grow slower, thus display resistance to antibiotics that are effective against actively dividing bacteria [3]. In *P. aeruginosa,* the biofilm matrix mainly consists of exopolysaccharide, secretory proteins, lipids and extracellular DNA (eDNA). The main exopolysaccharides of *P. aeruginosa* biofilm include alginate, Pel and Psl, each of which provides different physiological characteristics to the bacterial biofilm [4]. Alginate is responsible for the mucoid phenotype of *P. aeruginosa,* facilitating bacterial persistence, accumulation of nutrients and water in biofilm and adhesion to respiratory tract mucin. In addition, alginate synthesis is associated with biofilm maturation, microcolony formation and resistance to unfavorable conditions [5]. In contrast, Pel and Psl are responsible for biofilm initiation and maturation through facilitating intracellular adhesion and formation of surface-attached architecture [4].

Coumarin is a plant-derived bioactive compound made up of fused benzene and α-pyrone rings. It is a plant secondary metabolite that is found in leaves, roots and seeds of plants. Coumarins exhibit a wide range of pharmacological potency, such as anti-inflammatory, anticancer, and antibacterial, which are due to their ability to exert non-covalent interactions with organic macromolecules [6]. It has been documented that coumarin can exert antibacterial properties via different mechanisms, including quorum-sensing inhibition, biofilm inhibition and disruption, and growth inhibition. Furthermore, it can cause certain metabolic and gene expression alterations in pathogenic bacteria, which ultimately lead to a decrease in their virulence [7, 8]. However, like many other plant metabolites, coumarin lacks sufficient water solubility and bioavailability, which limits its biomedical applications [6]. For this reason, studies have focused on improving the bioavailability of this substance in order to improve its pharmaceutical potential.

A combination of nanomaterials with drugs and biomolecules provides several benefits, such as controlled drug release, protection against degradation and rapid clearance, and penetration and entrapment in biofilm matrix [9]. Therefore, using nanocarriers for the delivery of drugs and biomolecules to prevent and disrupt bacterial biofilm is an innovative strategy in antibacterial chemotherapy. Silver nanoparticles (Ag NPs) have been extensively studied for their antibacterial activity, as they are biocompatible, inexpensive and have significant antibacterial potential against a wide range of bacterial pathogens [10]. Ag NPs have received great attention for use as carriers for drug delivery to bacterial biofilms [11]. However, their potential for delivery of biomolecules, particularly coumarins, to prevent and eradicate bacterial biofilm has been less explored. Therefore, the current work was conducted to synthesize silver nanoparticles functionalized with D-glucose and conjugated with coumarin (Ag@Glu-Coumarin) and to characterize their antibacterial and antibiofilm potentials against MDR *P. aeruginosa* strains.

2. MATERIALS AND METHODS

2.1. Synthesis of Nanoparticles (NPs)

At first, Ag NPs (purchased from the US Research Nanomaterials Inc., USA) were functionalized with D-glucose using the following procedure to promote the conjugation of the NPs to coumarin (purchased from Merck, code 8.22316.0250, Germany). One gram of Ag NPs and 0.5 gram of D-glucose were dispersed using an ultrasonic water bath and then heated at 180 °C for 3 hours. The mixture was centrifuged at 6000 rpm and Ag@Glu NPs were collected and dried in an oven at 70 °C. To conjugate the NPs with coumarin, one gram of Ag@Glu NPs and one gram of coumarin (Sigma-Aldrich) were dispersed in 50 mL of distilled water and the reaction mixture was shaken for 24 hours at 25 °C. Finally, Ag@Glu-Coumarin NPs were collected using centrifugation, rinsed with distilled water and freeze-dried [12].

2.2. Characterization of the NPs

The physical and chemical properties of the NPs were characterized by Fourier Transform Infrared Spectroscopy (FT-IR), X-ray diffraction (XRD), Field Emission Scanning Electron Microscope (FE-SEM), Energy-dispersive X-ray spectroscopy (EDS), Dynamic Light Scattering (DLS), zeta potential and Thermogravimetric Assay (TGA) analyses. FT-IR analysis of Ag, coumarin and Ag@Glu-Coumarin NPs was performed using a Nicolet IR-100 FT-IR device in a wavenumber range of 500-4500 cm^{-1}. The assay was done to compare the functional groups of the substances. To determine the crystal structure of Ag@Glu-Coumarin, an XRD analysis was conducted using the Co- Ka X-radiation at k=1.79 Å. Field emission scanning electron microscopy (TESCAN Mira3 SEM) was employed to determine the shape and size of dried NPs, and an EDS-mapping assay was conducted to elucidate the atomic composition of the NPs. The surface charge and hydrodynamic size of Ag@Glu-Coumarin NPs in an aqueous environment were characterized using the DLS and zeta potential analyses (Malvern Ltd, 6.32 zeta sizer). Finally, Thermogravimetric Assay (TGA) was applied to determine the thermal stability of the NPs using a Rheometric Scientific STA 1500 (USA) device.

2.3. Bacterial Strains and Antibiogram

A total of 10 clinical *P. aeruginosa* strains and *P. aeruginosa ATCC 27853* were included in this work. The bacteria were isolated from clinical specimens (Shahid Motahari Hospital, Tehran, Iran) and identified using standard identification assays. To identify Multidrug-Resistant (MDR) strains, a standard antibiogram assay was applied using the ampicillin (10μg), ciprofloxacin (5μg), tetracycline (30μg), imipenem (10μg) and gentamicin (10μg) disks. In brief, a spread culture of the bacterial strains (1.5×10^8 CFU/mL) was prepared and the standard antibiotic disks were placed on the surface of the medium. The plate was incubated at 37 °C for 24 hours, after which

the zones of inhibition around the disks were measured [13].

2.4. Antibacterial Properties

The antibacterial effect of Ag nanoparticles (NPs), coumarin and Ag@Glu-Coumarin NPs on *P. aeruginosa* strains was studied by disk diffusion assay. In brief, a suspension of each bacterial strain with a density of 1.5 $\times 10^8$ CFU/mL was prepared and cultures of the strains were prepared over the Muller-Hinton Agar medium using sterile cotton swabs. Next, wells of 5 mm in diameter were punctured in the medium and 50 µL of the substances was added to the wells. A ciprofloxacin disk was also used as a standard antibiotic. The plate was incubated at 37 °C and zones of inhibition around the wells were measured [14].

2.5. Minimum Inhibitory Concentration (MIC)

To determine the Minimum inhibitory concentration (MIC) of Ag NPs, coumarin, Ag@Glu-Coumarin NPs and ciprofloxacin (as a standard drug), a gradient concentration of each substance ranging from 1 to 1024 µg/mL was prepared in a 96-well plate and bacterial stock (1.5 $\times 10^8$ CFU/mL) was added to the wells. The plate was incubated at 37 °C for 24 hours and then, bacterial growth was inspected based on the appearance of turbidity in each well. The minimum concentration of each substance that inhibited bacterial growth was regarded as MIC [15].

2.6. Antibiofilm Assay

Initially, the biofilm formation level of the strains was studied by the crystal violet staining method. In brief, the bacteria were grown in the Muller-Hinton Broth in a 96-well plate at 37 °C for 48 hours. After incubation, the medium was aspirated and gently rinsed with PBS to remove planktonic cells and the wells were stained with 0.1% crystal violet solution for 20 minute. The wells were washed with distilled water to remove the unbound dye and then 200µL of 30% acetic acid was added to the wells to solubilize the dye. Finally, the absorbance of each well was measured at 570 nm to quantify the biofilm level in each well [16].

To study the antibiofilm potential, the bacteria with the highest biofilm formation potential were selected for the antibiofilm assay. Initially, the bacteria were treated with a sub-MIC of Ag NPs, coumarin, and Ag@Glu-Coumarin NPs, at 37 °C for 48 hours, after which the biofilm level in each well was quantified by crystal violet staining assay, as described above.

2.7. Gene Expression

The expression level of the genes involved in the synthesis of biofilm exopolysaccharides, including *algD, pelA* and *pslA* was quantified using real-time PCR assay. In brief, the bacteria were treated with a sub-MIC of Ag NPs, coumarin and Ag@Glu-Coumarin NPs for 24 hours, while the untreated bacteria were considered the controls. Total RNA was initially extracted and complementary DNA (cDNA) was synthesized by Zist Virayesh cDNA synthesis kit, according to the manual. Finally, gene expression was done using an Ampliqon SYBR Green master mix in a Rotor-Gene QIAGEN thermocycler device. The *16s rRNA* gene was used as an internal control gene and gene expression levels were quantified using the $2^{-\Delta\Delta Ct}$ method [17]. The sequence of the primers used for gene amplification is provided in Table 1.

Table 1.
Sequence of the primers used for gene expression assay

Gene	Forward primer	Reverse primer	Product size (bp)
algD	5′-GGGCTATGTCGGTGCAGTAT-3′	5′-AACGATACGTCGGAGTCCAG-3′	219
pelA	5′-TACTGGGCCTCGAAGTTCTC-3′	5′-TCATCAAGCCCTATCCGTTC-3′	214
pslA	5′-GTTCTGCCTGCTGTTGTTCA-3′	5′-GGTTGCGTACCAGGTATTCG-3′	230
16s rRNA	5′-CCAACCCTTTTCCTTACTTGC-3′	5′-CATCAACTTCACCTTCACGC-3′	119

2.8. Statistical Analyses

The experiments were performed in triplicate and the results were presented as mean±standard deviation (SD). Significant differences between the treatment groups were investigated by one-way ANOVA and a p-value of less than 0.05 was considered statistically significant. To identify which specific groups differed, Tukey's post hoc analysis was subsequently performed.

3. RESULTS AND DISCUSSION

3.1. Characterization

In the FT-IR spectrum of Ag NPs, the peak at wavenumber of 567 cm^{-1} corresponds to the Ag bond and the peak at 3441 cm^{-1} is related to the O-H bond. Considering the spectrum and comparison with previous reports, it can be concluded that the results are consistent with other references and Ag NPs have been synthesized correctly [18, 19]. In the FT-IR spectrum of Ag@Glu-Coumarin NPs, the presence of a peak at 459 cm^{-1} is due to the Ag bond. Also, the presence of peaks at 753, 1116, 1395, 1605 and 1734 cm^{-1} is related to H-C, C-O, C-C, C=O, and C=C bonds, respectively. Also, the absorption peaks at 12926 and 3418 cm^{-1} are related to H-C, and O-H bonds, respectively. The FT-IR spectra were displayed in Fig. 1.

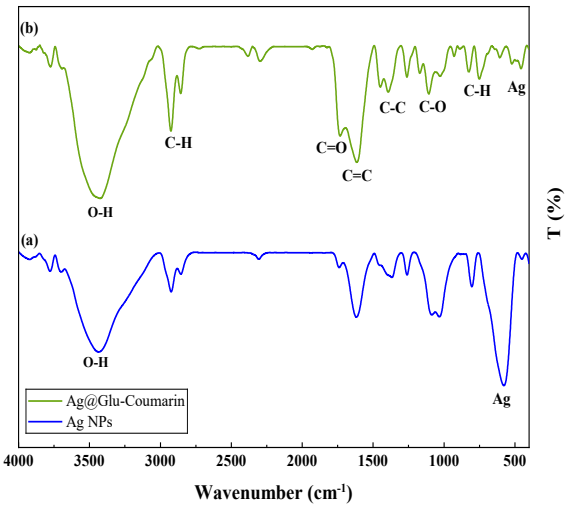

Fig. 1. FT-IR spectra of Ag and Ag@Glu-Coumarin NPs. The spectra display correct synthesis of the nanocomposite.

According to the XRD spectrum of Ag@Glu-Coumarin NPs, the peaks at 2θ of 38.18, 44.29, and 64.52 degrees are related to Ag NPs, which is in accordance with the card number 087-0719 from the Joint Committee on Powder Diffraction Standards (JCPDS) database and is in accordance with previous studies [18, 19]. According to the intensity of the peaks in this spectrum, it can be claimed that the material has a very high crystalline property. Also, the size of the nanoparticles from the Scherrer relationship is 3.89 nm. In the spectrum related to the Coumarin, the presence of peaks at 2θ of 11.40, 22.90, and 48.25 degrees is in accordance with previous research [20]. In the XRD spectrum of Ag@Glu-Coumarin, the presence of peaks at 2θ of 38.21, 44.45 and 64.45 degrees indicates the presence of silver NPs and at 2θ of 11.46, 22.97 and 48.30 degrees indicates the presence of coumarin. The structure of the composite is similar to the structure of its constituent materials (Fig. 2).

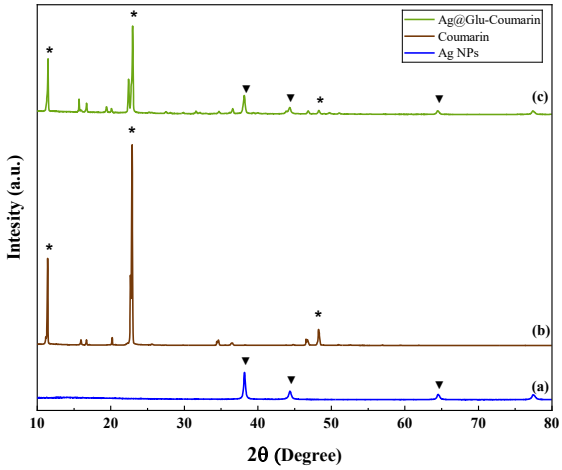

Fig. 2. XRD patterns of Ag NPs, Coumarin and Ag@Glu-Coumarin NPs. The structure of the nanocomposite is similar to the structure of its constituent materials.

According to FE-SEM, the nanoparticles were spherical and in a size range of 60 to 80 nm (Fig. 3a). Furthermore, no elemental impurity was noticed by EDS-mapping and the elemental composition of Ag@Glu-Coumarin NPs includes Ag (80.2 weight%), C (13.5 weight%) and O (6.3 weight%)(Fig. 3b). The surface charge and hydrodynamic size of Ag@Glu-Coumarin NPs in an aqueous solution were -80.4 mV and 271.2 nm, respectively, indicating well dispersion of the particles due to the high repulsion between the particles (Fig. 4). TGA analysis exhibited that Ag@Glu-Coumarin has sufficient thermal stability at temperatures up to 100 °C, which did not display considerable weight loss (Fig. 5).

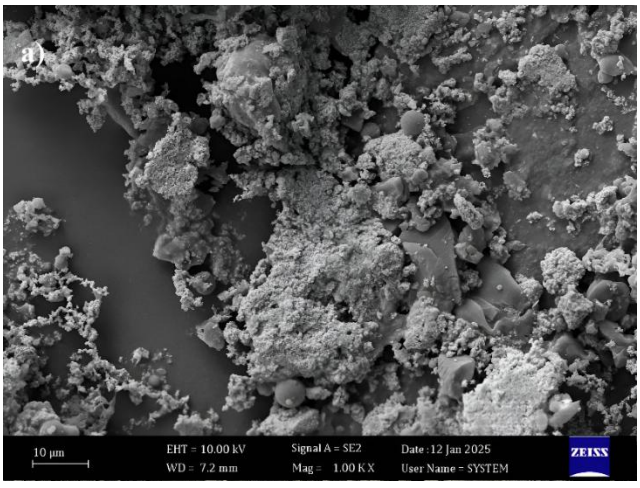

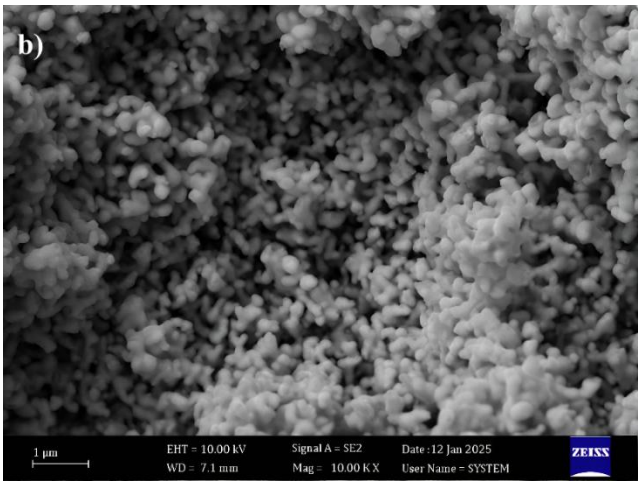

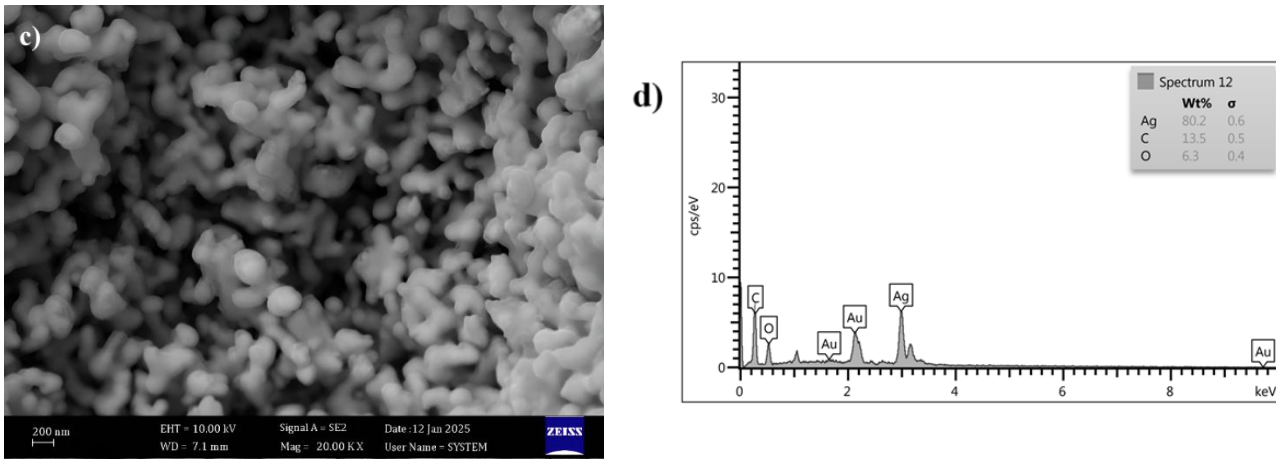

Fig. 3. FE-SEM (a,b,c) and EDS-mapping (d) of Ag@Glu-Coumarin NPs. The particles are spherical, in a nanoscale size range and contain no elemental impurities.

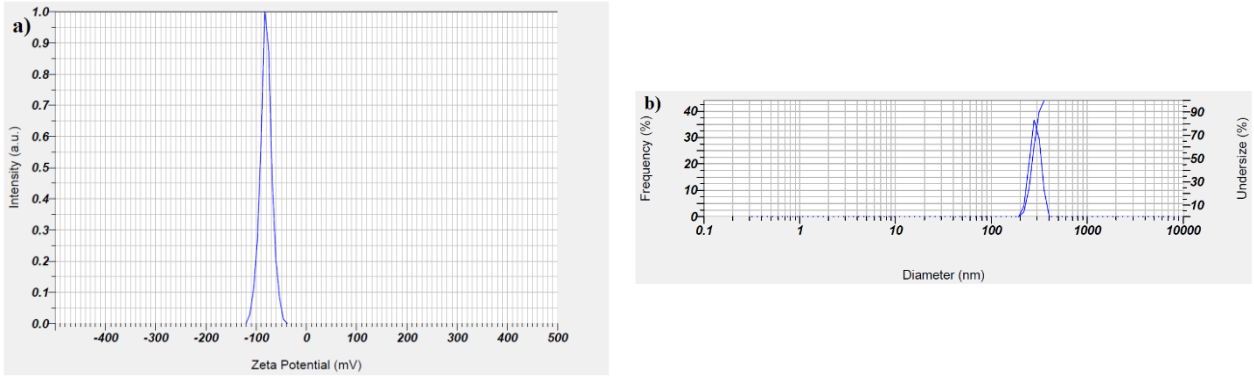

Fig. 4. Zeta potential (a) and DLS (b) of Ag@Glu-Coumarin NPs. The surface charge and hydrodynamic size of the NPs in an aqueous solution were -80.4 mV and 271.2 nm, respectively.

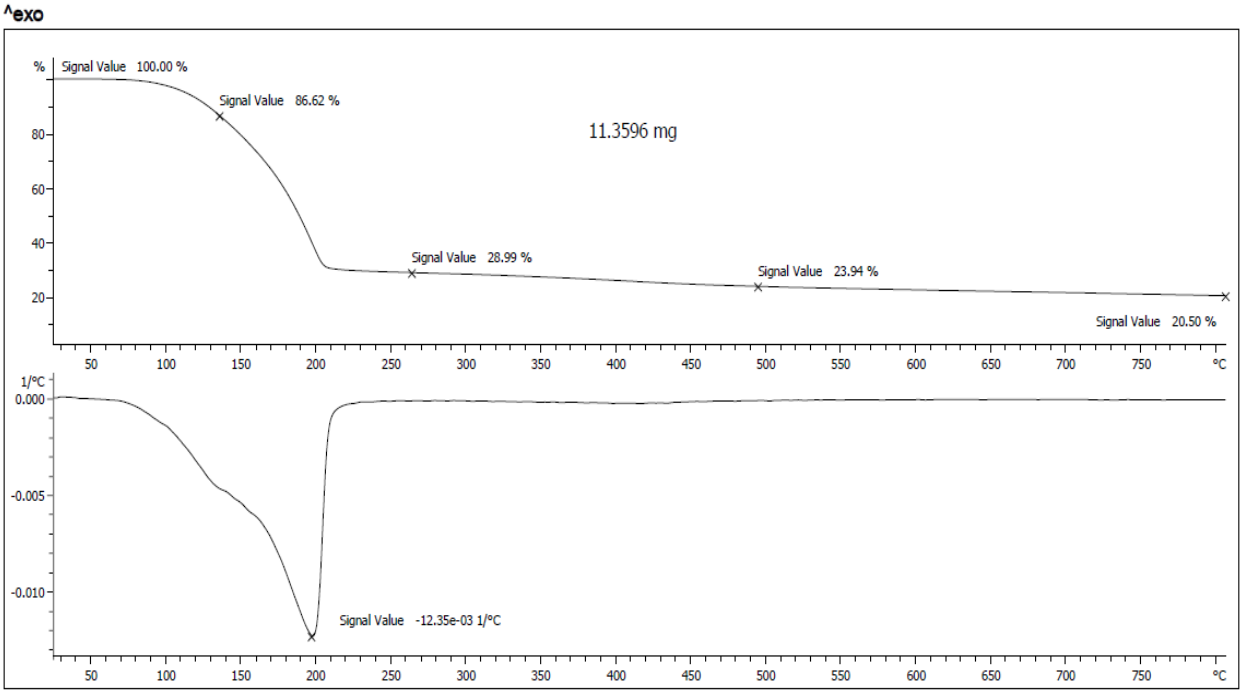

Fig. 5. TGA analysis of Ag@Glu-Coumarin NPs. The NPs have sufficient thermal stability at temperatures up to 100 °C and did not display considerable weight loss.

3.2. Antibiotic Resistance

Antibiogram assay for *P. aeruginosa* strains showed that the majority of strains were resistant to ampicillin (54.5%), followed by gentamicin (36.3%) and tetracycline (27.2%). In contrast, 63.3% of the strains were sensitive to ciprofloxacin and imipenem. Fig. 6 and Table 2 display the antibiotic resistance profile of the studied strains.

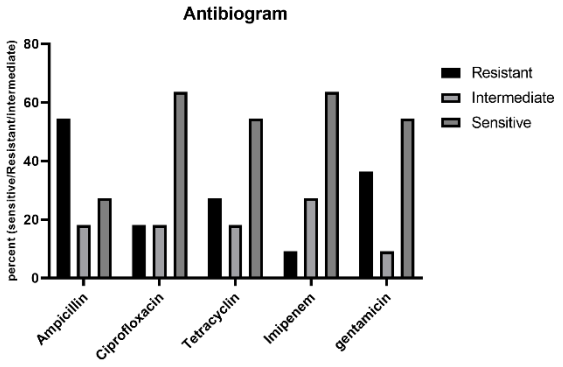

Fig. 6. Antibiogram of studied P. aeruginosa strains.

Table 2.
Antibiotic susceptibility profile of studied P. aeruginosa strain

***P. aeruginosa* strains**	**Ampicillin**	**Ciprofloxacin**	**Tetracyclin**	**Imipenem**	**gentamicin**
sample1	R	S	R	S	R
sample2	I	S	S	S	S
sample3	R	S	R	S	S
sample4	S	I	S	I	R
sample5	R	S	S	I	S
sample6	R	R	S	S	R
sample7	S	I	S	S	R
sample8	R	S	I	R	I
sample9	R	S	S	I	S
sample10	I	R	R	S	R
ATCC27853	S	S	I	S	S

3.3. Well-Diffusion Assay and MIC

According to the results, Ag@Glu-Coumarin NPs exhibited more antibacterial potency against *P. aeruginosa* strains than Ag and coumarin. The average diameter of zones of inhibition caused by Ag@Glu-Coumarin NPs, Ag NPs and coumarin was 30, 20 and 11.2 mm, respectively. The zone of inhibition of ciprofloxacin for the studied strains ranged 30.4 mm (Fig. 7).

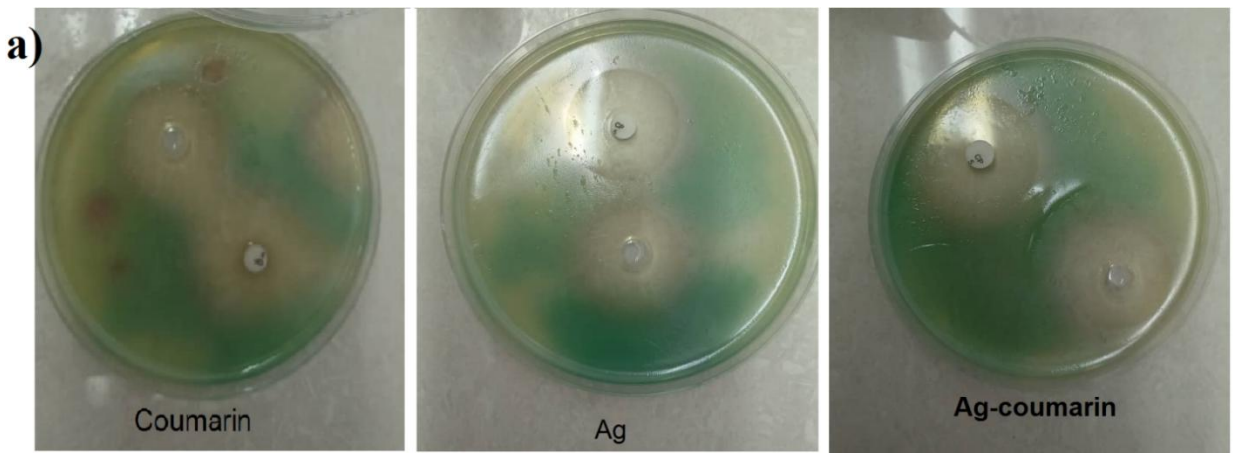

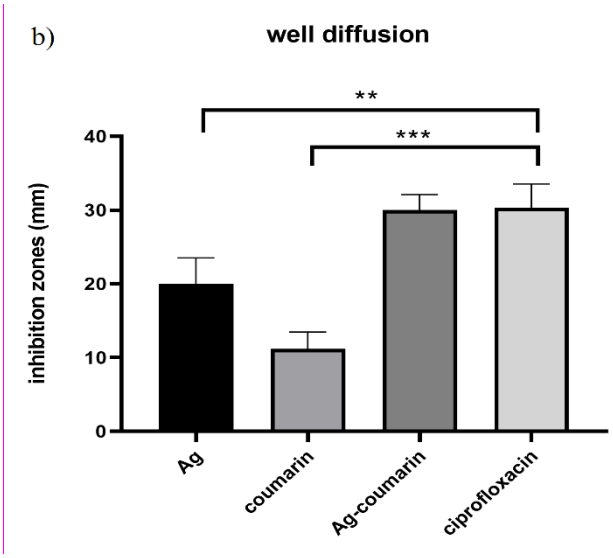

Fig. 7. Antibactarial potency of different substances against P. aeruginosa strains (a & b). Ag@Glu-Coumarin NPs exhibited stronger antibacterial effects on the studied strains than bare coumarin and Ag NPs.

The MIC of coumarin and Ag NPs for *P. aeruginosa* strains was 512-1024 µg/mL, while the MIC of Ag@Glu-Coumarin NPs for the studied strains ranged 256 to 512 µg/mL. In addition, the MIC of ciprofloxacin for clinical *P. aeruginosa* strains was 256-512 µg/mL and for *P. aeruginosa* ATCC 27853 was 128 µg/mL (Table 3).

Table 3.
MIC of different substances for studied P. aeruginosa strains

***P. aeruginosa* strain**	**MIC (µg/mL)**								**Average MIC (µg/mL)**			
	Ag-cumarin		**Ag**		**cumarin**		**ciprofloxacin**		**Ag-cumarin**	**Ag**	**cumarin**	**ciproflox acin**
sample1	512	512	1024	1024	1024	1024	512	512	512	1024	1024	512
sample2	256	256	1024	1024	512	512	512	512	256	1024	512	512
sample3	256	256	1024	1024	1024	1024	512	512	256	1024	1024	512
sample4	256	256	512	512	512	512	256	256	256	512	512	256
sample5	512	512	512	512	512	512	512	512	512	512	512	512
sample6	256	256	1024	1024	1024	1024	512	512	256	1024	1024	512
sample7	512	512	1024	1024	1024	1024	256	256	512	1024	1024	256
sample8	512	512	512	512	1024	1024	512	512	512	512	1024	512
sample9	256	256	512	512	512	512	512	512	256	512	512	512
sample10	512	512	1024	1024	1024	1024	512	512	512	1024	1024	512
ATCC:27853	512	512	512	512	512	512	128	128	512	512	512	128

3.4. Biofilm Formation/Inhibition Assay

According to the results, the strains 1, 6, 7, 8 and 10 displayed the highest biofilm formation levels with an average optical density (OD_{570}) of 1.41, 1.43, 1.53, 1.39 and 1.36, respectively. Treatment of the *P. aeruginosa* strains with Ag@Glu-Coumarin NPs resulted in the most robust biofilm inhibition, followed by coumarin and Ag NPs. The average OD_{570}, which corresponds to biofilm biomass in the bacteria treated with Ag@Glu-Coumarin NPs and coumarin, was 0.222 and 0.285, respectively, while the average absorbance in the Ag treatment group was 0.339. In other words, following treatment of strains 1, 6, 7, 8 and 10 with Ag@Glu-Coumarin NPs, the biofilm formation was inhibited by 77.3, 75.9, 90.3, 89.2 and 89.4%, respectively. In addition, biofilm formation of *P. aeruginosa* ATCC 27853 was reduced by 92.6%. The results indicate the efficient antibiofilm potential of Ag@Glu-Coumarin NPs against biofilm-producing MDR *P. aeruginosa* strains. The results were displayed in Fig. 8.

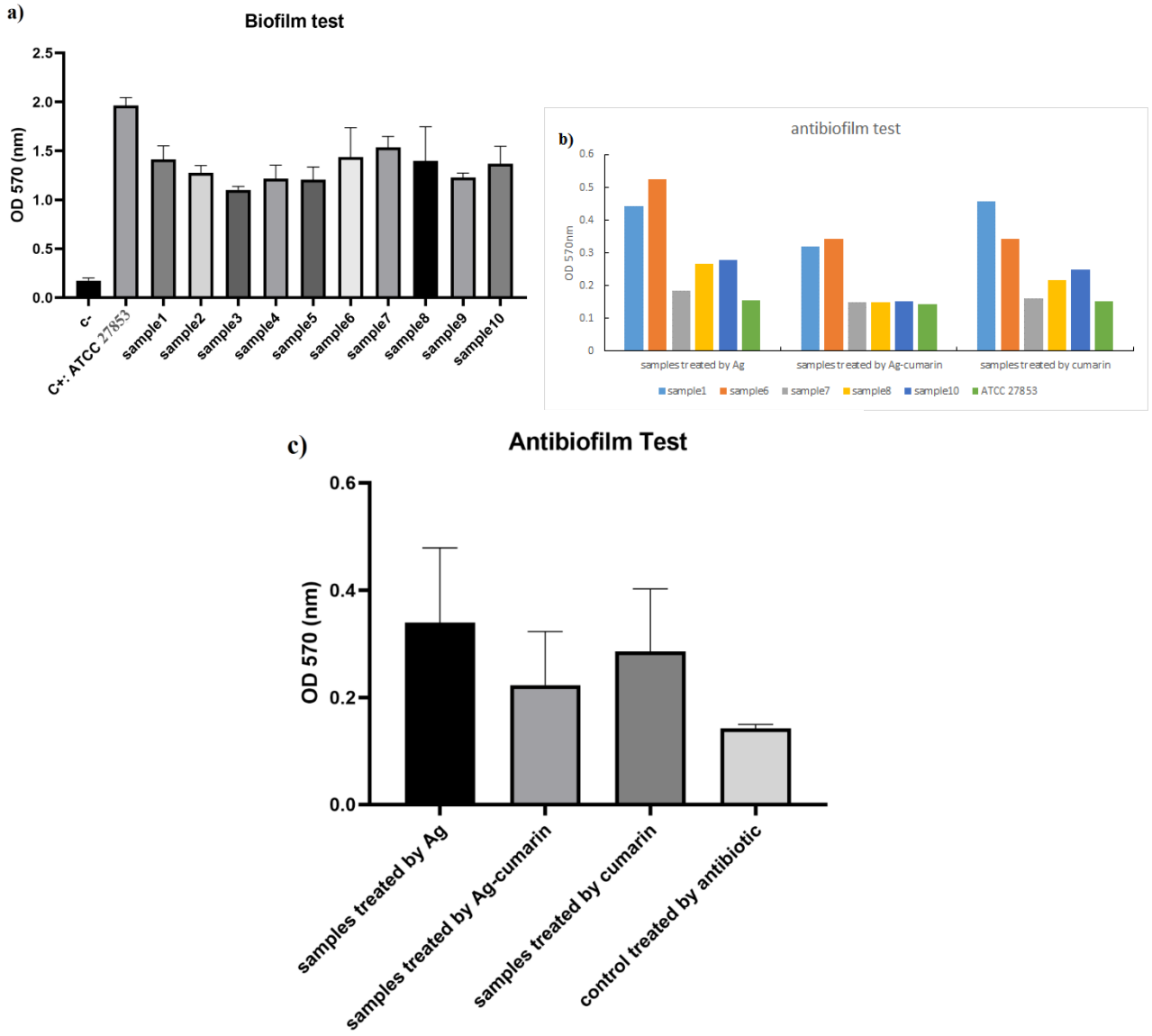

Fig. 8. Biofilm formation level of P. aeruginosa strains (a). Antibiofilm effects of Ag@Glu-Coumarin, coumarin and Ag NPs on selected P. aeruginosa strains (b&c). The results indicate the higher antibiofilm potential of Ag@Glu-Coumarin NPs than Ag NPs and coumarin.

3.5. Gene Expression

Real-time PCR assay showed that treatment of *P. aeruginosa* with Ag@Glu-Coumarin NPs caused a significant reduction in the expression of the gene involved in the synthesis of biofilm exopolysaccharides. The expression of *algD* in this treatment group was significantly reduced to 0.68-fold relative to the control, while Ag NPs and coumarin reduced the expression of this gene to 0.81 and 0.75 folds relative to the control, respectively (Fig. 9a).

Moreover, the average expression level of the *pelA* gene in the bacteria treated with Ag NPs and coumarin reduced to 0.68-fold and 0.76-fold relative to the control, respectively, while treatment of *P. aeruginosa* strains with Ag@Glu-Coumarin NPs resulted in the significant reduction of the *pelA* gene to 0.46-fold relative to the control (Fig. 9b).

A similar pattern was also observed for the expression of the *pslA* gene. The expression of this gene in bacteria treated with Ag@Glu-Coumarin NPs significantly decreased to 0.37-fold relative to the control, while Ag NPs and coumarin reduced gene expression to 0.81-fold and 0.47-fold relative to the control, respectively (Fig. 9c).

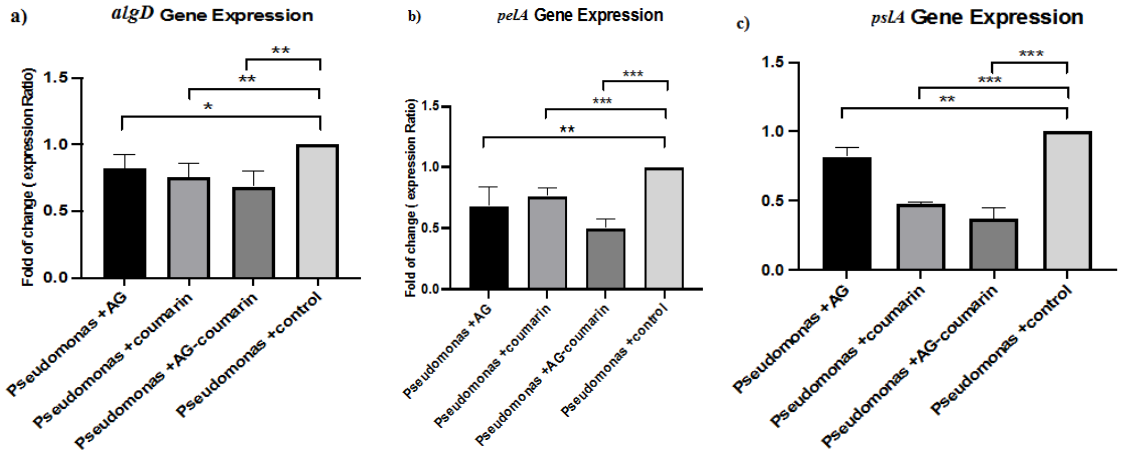

Fig. 9. Relative expression of the algD (a), pelA (b) and pslA (c) gene in P. aeruginosa strains after treatment with Ag NPs, coumarin and Ag@Glu-Coumarin NPs. Ag@Glu-Coumarin NPs caused significant reduction all studied genes.

Infections caused by MDR *P. aeruginosa* are a critical health challenge, particularly in hospital settings. In addition to the intrinsic and acquired resistance mechanisms, biofilm formation is regarded as a major contributing determinant in the development of MDR phenotype in *P. aeruginosa.* The polysaccharide matrix of the biofilm plays a crucial role in the failure of antibiotic efficacy on this pathogen. The use of metal nanoparticles is a promising approach to penetrate the biofilm matrix and deliver drugs and bioactive molecules to bacterial cells. Accordingly, the present study investigated the antimicrobial and antibiofilm effects of Ag@Glu-Coumarin NPs on MDR *P. aeruginosa*.

Characterization of the physicochemical properties of Ag@Glu-Coumarin NPs showed that the particles were correctly synthesized, contained no impurities and were at the nanoscale. Size is the main physicochemical determinant in the antibacterial potential of silver NPs, as it can affect the intrinsic antibacterial property and cellular uptake of the particles [21]. The small size of the particles can facilitate their penetration into the biofilm matrix, where they can exert their antibacterial effects more efficiently than large particles. Beyond size, shape can also affect the antibacterial activity of NPs, as it determines the contact between the nanomaterial and bacterial cell components. It has been documented that spherical silver NPs have good antibacterial potential due to high surface reactivity [22]. We found that the particles are strongly negatively charged, which provides sufficient repulsion between the particles to avoid particle agglomeration. Furthermore, we found that the particle size was increased in the aqueous medium compared to the dry form, which could be a result of water absorption and swelling.

Characterization of the antibacterial properties revealed that Ag@Glu-Coumarin NPs demonstrated antibacterial activity than bare Ag NPs and coumarin, suggesting additive antibacterial effects caused by Ag and coumarin. The antibacterial mechanism of silver mainly relies on the generation of reactive oxygen species (ROS) such as peroxide and superoxide ions, which can interact with bacterial cells, causing damage to cell components. It has been reported that the ROS molecules can cause damage to the bacterial cytoplasmic membrane, causing perturbation of its selective permeability and leakage of cytoplasmic content. In addition, the cytoplasmic membrane is a vital component of bacterial cells that regulates vital functions such as energy production, chemotaxis, and sensory transduction. Therefore, damage to the cytoplasmic membrane can disrupt essential cellular processes and inhibit or reduce bacterial growth. In addition, following the release of Ag ions from the synthesized NPs, they can interact with bacterial biomolecules, especially enzymes and DNA, and thus disrupt their normal function [21, 23]. Furthermore, the NPs can disrupt the normal functions of *P. aeruginosa* efflux systems, causing increased susceptibility of bacteria to antimicrobials [24]. The efflux systems are membrane-anchored proteins involved in the active extrusion of antibiotics and antibacterial molecules from bacterial cytoplasm, reducing their cytoplasmic concentration and developing bacterial resistance. It has been found that silver nano-conjugates can cause disruption of *P. aeruginosa* efflux systems which complies with our findings [25, 26]. Therefore, the inhibition of bacterial efflux pumps can be the underlying mechanism for antibacterial effects of Ag@Glu-Coumarin NPs than bare Ag NPs and coumarin.

In addition to the efflux systems, the outer membrane of *P. aeruginosa* is another intrinsic determinant for bacterial drug resistance. Due to the low permeability, it works as a barrier to the majority of antibacterial agents [27]. The oxidative damage due to the generation of ROS can be another contributing factor causing the sensitivity of *P. aeruginosa* to Ag@Glu-Coumarin NPs. Damage to the bacterial outer membrane can facilitate penetration of the generated ROS, Ag ions and Ag@Glu-Coumarin NPs into the bacterial cell, where they can exert additional antibacterial functions.

In addition to silver, coumarin has its antibacterial effects on *P. aeruginosa* strains. As reported in the previous studies, the antibacterial action of coumarin is primarily attributed to its ability to interact with bacterial DNA topoisomerase enzymes and inhibit bacterial secondary DNA structure [7, 28]. Therefore, Ag@Glu-Coumarin NPs can exert an additive antibacterial effect

through different mechanisms. By characterizing the antibiofilm potential, we found that Ag@Glu-Coumarin NPs were considerably more potent antibiofilm agents than Ag and coumarin against MDR *P. aeruginosa* strains. The inhibition of the bacterial biofilm can be associated with affecting bacterial quorum sensing (QS) and C-di-GMP (Guanosine monophosphate) levels by coumarin [8]. QS is a cell-to-cell communication mechanism based on the secretion of specific signal molecules, which regulate various cell functions, particularly virulence factors, drug resistance and biofilm formation [29]. Several QS systems have been found in *P. aeruginosa* that are involved in the regulation of biofilm formation. Therefore, QS inhibition is a promising anti-virulence strategy against *P. aeruginosa*. Coumarin has been described as a natural QS inhibitor in several pathogenic bacteria, including *P. aeruginosa*. Previous studies have reported that coumarin derivatives can interfere with QS systems of *P. aeruginosa*, causing inhibition of bacterial biofilm formation, which is in agreement with our findings [30].

C-di-GMP is considered an intracellular secondary messenger involved in the regulation of several functions in *P. aeruginosa*, including the synthesis of exopolysaccharides and biofilm formation [31]. It has been found that coumarin can interfere with the C-di-GMP metabolism, thereby reducing its intracellular content and interfering with its subsequent regulatory mechanisms. Therefore, in addition to QS inhibition, coumarin can perturb bacterial biofilm inhibition by reduction of C-di-GMP levels and these combined effects may explain the reduced biofilm levels observed in this work [8].

In agreement with biofilm inhibition, we observed that the expression of the genes involved in the expression of biofilm matrix polysaccharides significantly decreased by Ag@Glu-Coumarin NPs. The synthesis of alginate, Psl and Pel is regulated by the QS system of *P. aeruginosa*, particularly the Las QS system [32]. Therefore, the reduced expression of the *algD*, *pslA* and *pelA* that were observed in this work can be a result of the QS inhibitory effects of coumarin. Furthermore, several studies reported that generation of the Psl and Pel polysaccharides is highly dependent on the intracellular C-di-GMP level. Therefore, the reduced expression of the *pelA* and *pslA* may be associated with the reduction of C-di-GMP level by coumarin [33].

4. CONCLUSION

In this study, we observed that Ag@Glu-Coumarin NPs demonstrated antibacterial activity against MDR *P. aeruginosa* strains because the average diameter of zones of inhibition caused by Ag@Glu-Coumarin NPs was 30 mm and the MIC of Ag@Glu-Coumarin NPs for the studied strains ranged 256 to 512 µg/mL. The antibiofilm effects of Ag@Glu-Coumarin NPs against MDR *P. aeruginosa* strains were demonstrated. Following treatment of strains 1, 6, 7, 8 and 10 with Ag@Glu-Coumarin NPs, biofilm formation was inhibited by 77.3%, 75.9%, 90.3%, 89.2% and 89.4%, respectively. Also, Ag@Glu-Coumarin NPs efficiently reduce the expression of the biofilm exopolysaccharide genes. The expression of *algD* in this treatment group was significantly reduced to 0.68-fold relative to the control. This work increased our understanding of the antibacterial mechanism of coumarin nanocomplexes and suggests their therapeutic potential against the MDR *P. aeruginosa* strain. For this purpose toxicity toward mammalian cells should be evaluated using MTT assay. However, the lack of more detailed molecular characterization and in-vivo infection models is a limitation of this work, which need to be considered in future studies.

ACKNOWLEDGEMENT

We gratefully acknowledge the support of Islamic Azad University, Rasht Branch, Rasht, Iran.

CONFLICT OF INTEREST

The authors declare that there are no conflicts of interest regarding this article.

REFERENCES

[1] Sathe N, Beech P, Croft L, Suphioglu C, Kapat A, Athan E. Pseudomonas aeruginosa: infections and novel approaches to treatment ‘Knowing the enemy’ the threat of Pseudomonas aeruginosa and exploring novel approaches to treatment. Infect Med. 2023;2(3):178–194. doi:10.1016/j.imj.2023.05.003.

[2] Kunz CAJ, El Ghali A, Holger D, Rebold N, Rybak MJ. Therapeutic strategies for emerging multidrug-resistant Pseudomonas aeruginosa. Infect Dis Therapy. 2022;11(2):661–682. doi:10.1007/s40121-022-00591-2.

[3] Fernández-Billón M, Llambías-Cabot AE, Jordana-Lluch E, Oliver A, Macià MD. Mechanisms of antibiotic resistance in Pseudomonas aeruginosa biofilms. Bioflm. 2023;5:100129. doi:10.1016/j.bioflm.2023.100129.

[4] Sharma G, Rao S, Bansal A, Dang S, Gupta S, Gabrani R. Pseudomonas aeruginosa biofilm: potential therapeutic targets. Bio. 2014;42(1):1–7. doi:10.1016/j.biologicals.2013.11.001.

[5] Tan Y, Dai Z. Pseudomonas aeruginosa mucinous phenotypes and algUmucABD operon mutant characteristics obtained from inpatients with bronchiectasis and their correlation with acute aggravation. Front Cell Infect Microbiol. 2024;14:1402348. doi:10.3389/fcimb.2024.1402348.

[6] Yadav AK, Shrestha RM, Yadav PN. Anticancer mechanism of coumarin-based derivatives. Europ J Med Chem. 2024;267:116179. doi:10.1016/j.ejmech.2024.116179.

[7] Mustafa YF. Emerging trends and future opportunities for coumarin-heterocycle conjugates as antibacterial agents. Res Chem. 2023;6:101151. doi:10.1016/j.rechem.2023.101151.

[8] Zhang Y, Sass A, Van Acker H, Wille J, Verhasselt B, Van Nieuwerburgh F, et al. Coumarin reduces virulence and biofilm formation in Pseudomonas aeruginosa by affecting quorum sensing, type III secretion and C-di-GMP levels. Front Microbiol. 2018;9:1952. doi:10.3389/fmicb.2018.01952.

[9] Dos Santos Ramos MA, Da Silva PB, Spósito L, De Toledo LG, Bonifacio BV, Rodero CF, et al. Nanotechnology-based drug delivery systems for control of microbial biofilms: a review. Int J Nanomed. 2018:1179–1213. doi:10.2147/IJN.S146195.

[10] Wypij M, Jedrzejewski T, Trzcinska-Wencel J, Ostrowski M, Rai M, Golinska P. Green synthesized silver nanoparticles: antibacterial and anticancer activities, biocompatibility, and analyses of surface-attached proteins. Front Microbiol. 2021;12:632505. doi:10.3389/fmicb.2021.632505.
[11] Ravindra S, Mulaba-Bafubiandi AF, Rajinikanth V, Varaprasad K, Narayana Reddy N, Mohana Raju K. Development and characterization of curcumin loaded silver nanoparticle hydrogels for antibacterial and drug delivery applications. J Inorg Organom Pol Mat. 2012;22:1254–1262. doi:10.1007/s10904-012-9734-4.
[12] Shokrollahi F, Salehzadeh A, Kafilzadeh F, Zaefizadeh M. Evaluation the effect of iron oxide nanoparticles functionalized by glucose and conjugated with coumarin (Fe3O4@ Glu-coumarin NPs) on expression of CASP8, CASP9, p53, mTOR1, and MAPK1 genes in liver cancer cell line. Gen Rep. 2023;33:101818. doi:10.1016/j.genrep.2023.101818.
[13] Hudzicki J. Kirby-Bauer disk diffusion susceptibility test protocol. Americ Soci Microbiol. 2009;15(1):1–23.
[14] Kora AJ, Arunachalam J. Assessment of antibacterial activity of silver nanoparticles on Pseudomonas aeruginosa and its mechanism of action. Wrld J Microbiol Biotech. 2011;27:1209–1216. doi:10.1007/s11274-010-0569-2.
[15] Parvekar P, Palaskar J, Metgud S, Maria R, Dutta S. The minimum inhibitory concentration (MIC) and minimum bactericidal concentration (MBC) of silver nanoparticles against Staphylococcus aureus. Bio Inv Dent. 2020;7(1):105–109. doi:10.1080/26415275.2020.1796674.
[16] Shao X, Xie Y, Zhang Y, Deng X. Biofilm formation assay in Pseudomonas syringae. Bio-protocol. 2019;9(10):e3237–e3237. doi:10.21769/BioProtoc.3237.
[17] Pfaffl MW. A new mathematical model for relative quantification in real-time RT–PCR. Nucleic Acids Res. 2001;29(9):e45–e45. doi:10.1093/nar/29.9.e45.
[18] Idris DS, Roy A. Antioxidant and dye degradation activity of green synthesized silver-iron oxide (Ag-Fe2O3) bimetallic nanoparticles. Nano-Struc Nano-Obj. 2024;38:101142. doi:10.1016/j.nanoso.2024.101142.
[19] Meydan I, Seckin H, Kocak Y, Okumus E, Bekmezci M, Sen F. Evaluation of antioxidant, antibacterial and thermal stability properties of silver nanoparticles synthesised with Infundibulicybe gibba extract. Int J Enviro Sci Tech. 2025;22(8):6957–6966. doi:10.1007/s13762-024-06131-4.
[20] Stefanou V, Matiadis D, Tsironis D, Igglessi-Markopoulou O, McKee V, Markopoulos J. Synthesis and single crystal X-ray diffraction studies of coumarin-based Zn (II) and Mn (II) complexes, involving supramolecular interactions. Polyhedron. 2018;141:289–295. doi:10.1016/j.poly.2017.12.011.
[21] Menichetti A, Mavridi-Printezi A, Mordini D, Montalti M. Effect of size, shape and surface functionalization on the antibacterial activity of silver nanoparticles. J Func Biomat. 2023;14(5):244. doi:10.3390/jfb14050244.
[22] Hong X, Wen J, Xiong X, Hu Y. Shape effect on the antibacterial activity of silver nanoparticles synthesized via a microwave-assisted method. Enviro Sci Poll Res. 2016;23:4489–4497.
[23] Xu L, Wang YY, Huang J, Chen CY, Wang ZX, Xie H. Silver nanoparticles: synthesis, medical applications and biosafety. Theranostics. 2020;10(20):8996. doi:10.7150/thno.45413.
[24] Gupta D, Singh A, Khan AU. Nanoparticles as efflux pump and biofilm inhibitor to rejuvenate bactericidal effect of conventional antibiotics. Nanosca Res Let. 2017;12:1–6. doi:10.1186/s11671-017-2222-6.
[25] Nallathamby PD, Lee KJ, Desai T, Xu XHN. Study of the multidrug membrane transporter of single living Pseudomonas aeruginosa cells using size-dependent plasmonic nanoparticle optical probes. Biochem. 2010;49(28):5942–5953. doi:10.1021/bi100268k.
[26] Abdolhosseini M, Zamani H, Salehzadeh A. Synergistic antimicrobial potential of ciprofloxacin with silver nanoparticles conjugated to thiosemicarbazide against ciprofloxacin resistant Pseudomonas aeruginosa by attenuation of MexA-B efflux pump genes. Biol. 2019;74:1191–1196. doi:10.2478/s11756-019-00269-0.
[27] Langendonk RF, Neill DR, Fothergill JL. The building blocks of antimicrobial resistance in Pseudomonas aeruginosa: implications for current resistance-breaking therapies. Front Cell Infect Microbiol. 2021;11:665759. doi:10.3389/fcimb.2021.665759.
[28] Feng D, Zhang A, Yang Y, Yang P. Coumarin-containing hybrids and their antibacterial activities. Archiv Pharm. 2020;353(6):1900380. doi:10.1002/ardp.201900380.
[29] Whiteley M, Diggle SP, Greenberg EP. Progress in and promise of bacterial quorum sensing research. Nature. 2017;551(7680):313–320. doi:10.1038/nature24624.
[30] Tajani AS, Tehranizadeh ZA, Pourmohammad A, Iranshahi M, Farhadi F, et al. Anti-quorum sensing and antibiofilm activity of coumarin derivatives against Pseudomonas aeruginosa PAO1: insights from in vitro and in silico studies. Iranian J Basic Med Sci. 2023;26(4):445. doi:10.22038/IJBMS.2023.69016.15047.
[31] Valentini M, Filloux A. Biofilms and cyclic di-GMP (c-di-GMP) signaling: lessons from Pseudomonas aeruginosa and other bacteria. J Bio Chem. 2016;291(24):12547–12555. doi:10.1074/jbc.R115.711507.
[32] Liu Q, Wu Q, Liu J, Xu T, Liu J, Wu Q, et al. New insights into the mediation of biofilm formation by three core extracellular polysaccharide biosynthesis pathways in Pseudomonas aeruginosa. Int J Mole Sci. 2025;26(8):3780. doi:10.3390/ijms26083780.
[33] Ha DG, O'Toole GA. c-di-GMP and its effects on biofilm formation and dispersion: a Pseudomonas aeruginosa review. Microbial Biofilms. 2015:301–317. doi:10.1128/9781555817466.ch15.